Bioconjugate Chemistry

Article

pubs.acs.org/bc

Mass Spectrometric Characterization of Transglutaminase Based Site-Specific Antibody–Drug Conjugates

Santiago E. Farias, Pavel Strop,* Kathy Delaria, Meritxell Galindo Casas, Magdalena Dorywalska, David L. Shelton, Jaume Pons, and Arvind Rajpal

Rinat-Pfizer Inc., 230 East Grand Avenue, South San Francisco, California 94080, United States

Supporting Information

ABSTRACT: Antibody drug conjugates (ADCs) are becoming an important new class of therapeutic agents for the treatment of cancer. ADCs are produced through the linkage of a cytotoxic small molecule (drug) to monoclonal antibodies that target tumor cells. Traditionally, most ADCs rely on chemical conjugation methods that yield heterogeneous mixtures of varying number of drugs attached at different positions. The potential benefits of site-specific drug conjugation in terms of stability, manufacturing, and improved therapeutic index has recently led to the development of several new site-specific conjugation technologies. However, detailed characterization of the degree of site specificity is currently lacking. In this study we utilize mass spectrometry to characterize the extent of site-specificity of an enzyme-based site-specific antibody–drug conjugation technology that we recently developed. We found that, in addition to conjugation of the engineered site, a small amount of aglycosylated antibody present in starting material led to conjugation at position Q295, resulting in approximately 1.3% of off-target conjugation. Based on our detection limits, we show that Q295N mutant eliminates the off-target conjugation yielding highly homogeneous conjugates that are better than 99.8% site-specific. Our study demonstrates the importance of detailed characterization of ADCs and describes methods that can be utilized to characterize not only our enzyme based conjugates, but also ADCs generated by other conjugation technologies.

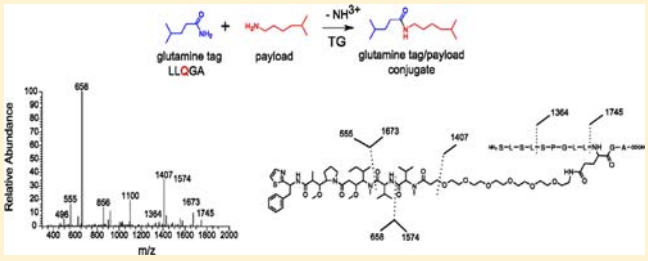

INTRODUCTION

Antibody drug conjugates (ADCs) have emerged as an important class of therapeutic agents in the treatment of cancer with increased antitumor efficacy and reduced toxicity when compared to classic chemotherapy.[1−5] ADCs are produced through a covalent linkage of a cytotoxic small molecule (drug) to monoclonal antibodies that recognize antigens on the surface of cancer cells.[6−9] Traditionally, most ADCs rely on chemical conjugation methods where a chemotherapeutic agent is linked to lysines or cysteines on the antibody.[6,10,11] In general, these conjugates are heterogeneous mixtures of a varying number of drugs attached at different positions throughout the antibody.[12,13]

To avoid unfavorable characteristics of ADCs heterogeneity such as variable stability[14−16] and manufacturing inconsistency, considerable effort in the ADC field has been focused on developing site-specific conjugation technologies to produce more stoichiometrically controlled and homogeneous ADCs.[2,17−21] While the superiority of site-specific conjugation has yet to be demonstrated in the clinic, one can hypothesize that through careful selection of the conjugation site it may be possible to tune the pharmacokinetics, efficacy, and safety properties of ADCs, and thereby obtain a better therapeutic window. For instance, Junutula et al. demonstrated that site-specific ADCs can improve therapeutic index in animal models.[22] For these reasons, many approaches to obtain site-specific antibody–drug conjugates are now being explored. These efforts include the development of engineered cysteines and incorporation of unnatural amino acids.[22,23]

We developed an alternative site-specific conjugation approach that utilizes the transglutaminase (TG) enzyme from *Streptoverticillium mobaraense*.[17] Similar to mammalian TG, microbial TG catalyzes the formation of a covalent bond between a glutamine side chain and a primary amine[24,25] (Figure 1a). Conjugation with mTG was previously employed to PEGylate proteins and to create radioimmuno conjugates.[26,27] In order to produce site-specific ADCs using transglutaminase technology we incorporated a glutamine tag (LLQGA) in a surface accessible region of an antibody and linked the glutamine in the tag to a cytotoxic drug that contains a primary amine on the linker. Optimal conjugation positions were found by introducing engineered glutamine tags at surface accessible regions of an antibody and testing conjugation efficiency. As a result, we identified several conjugation positions that conveyed optimal conjugation efficiency while retaining favorable antibody biophysical properties. While site-specific conjugation is becoming increasingly popular for ADCs, relatively little has been published in terms of

Received: August 20, 2013
Revised: December 10, 2013
Published: December 20, 2013

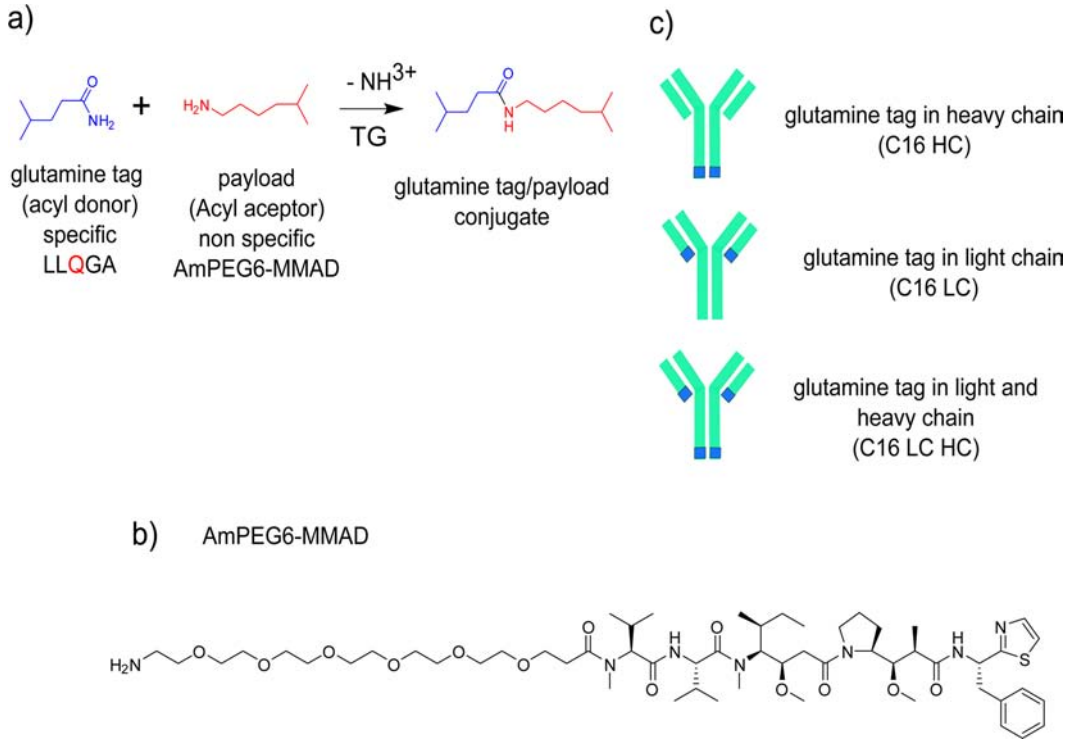

Figure 1. mTG catalyzed site-specific conjugation of antibody–drug conjugates. (a) Chemical reaction catalyzed by mTG. (b) AmPEG6-MMAD payload. (c) Positions of glutamine tags in antibody that can be conjugated at high yields.

Table 1. AmPEG6-MMAD Conjugated Peptides in C16 HC, C16 LC, and C16 LC HC

	sequence	retention time (min)	observed mass (Da)	theoretical mass (Da)	error (ppm)
C16 HC	SLSLSPGLLQ*GA	70.52	2331.2793	2331.2864	3
	EEQ*YNSTYR	59	2278.1591	2278.1568	1
C16 HC Q295N	SLSLSPGLLQ*GA	70.11	2331.275	2331.286	5
C16 LC	GECGGLLQ*GA	67	2050.0785	2050.0856	3.5
	SFNRGECGGLLQ*GA	63.57	2553.3247	2553.3217	1.2
	EEQ*YNSTYR	59.1	2278.1545	2278.1568	1
C16LC	GECGGLLQ*GA	67	2050.0737	2050.0856	5.8
Q295N	SFNRGECGGLLQ*GA	63.50	2553.3219	2553.3217	0.1
C16 LC HC	SLSLSPGLLQ*GA	70.09	2331.2729	2331.2864	5.7
	EEQ*YNSTYR	59	2278.1511	2278.1568	2.5
	GECGGLLQ*GA	67.03	2050.0741	2050.0856	5.6
	SFNRGECGGLLQ*GA	63.69	2553.3208	2553.3217	0.4

characterizing the degree of specificity afforded by a given conjugation methodology. The best-described site-specific ADC has been a conjugate of cleavable MMAE (maleimide caproyl–Valine Citruline–PABC–monomethyl auristatin E) to an engineered cysteine in the heavy chain of an antibody.[3,22] LC/MS analysis of the fragment antigen binding (Fab) fragment cleaved from this ADC identified MMAE conjugated tryptic peptides using a signature in-source fragmentation ion observed in the mass spectra of drug containing peptides. The four most intense ions were identified as complete or partial tryptic cleavage fragments located around the engineered cysteine. Recently Dai et al. also described a work flow to characterize sites of bioconjugation by immune-affinity capture coupled to MALDI-TOF mass spectrometry.[28]

In this study we characterized the transglutaminase based site-specific linkage of the amino-polyethylene glycol-6 propionyl monomethyl auristatin D (AmPEG6-MMAD) payload (Figure 1b) to engineered glutamine tags in the C-terminus of heavy chain (C16 HC), C-terminus of light chain (C16 LC), and to an antibody containing tags in both the light and heavy chains (C16 LC HC) by high-resolution mass spectrometry (Figure 1c, Table 1). To characterize the extent of site specificity, we utilized a combination of intact mass, high-resolution peptide mapping (LC-MS and LC-MS/MS) and in-source fragmentation analysis. In addition, we generated standard curves for quantification purposes using conjugated peptide standards spiked into unconjugated antibody tryptic digests. We found that traces of aglycosylated antibody present in the starting material leads to approximately 1.3% of off-target conjugation. Based on our detection limits, we also show that Q295N mutant eliminates the off-target conjugation yielding highly homogeneous conjugates that are more than 99.8% site-specific.

dx.doi.org/10.1021/bc4003794 | *Bioconjugate Chem.* 2014, 25, 240–250

MATERIALS AND METHODS

LC/MS Intact Mass Analysis of ADC. Prior to LC/MS analysis, ADCs and antibodies were deglycosylated with PNGase F (NEB, cat #P0704L) under nondenaturing conditions at 37 °C overnight. For light chain and heavy chain analysis, samples were reduced with dithiothreitol (DTT) 20 mM final concentration for 30 min at 60 °C after deglycosylation. ADCs (500 ng) were loaded into a reverse phase column packed with a polymeric material (Michrom-Bruker, cat #CM8/00920/00). LC/MS analysis was performed using Agilent 1100 series HPLC system, comprising binary HPLC pump, degasser, thermostatted auto sampler, column heater, and diode-array detector (DAD), coupled to an Orbitrap Velos Pro (Thermo Scientific) mass spectrometer with electrospray ion source. The resulting mass spectra were deconvoluted using ProMass software (Thermo Fisher Scientific).

Relative Quantitation of ADC by Intact Mass. Before intact mass analysis, conjugated and unconjugated C16 HC were deglycosylated with PNGase F (NEB, cat #P0704L) under nondenaturing conditions at 37 °C overnight. A total of 1 μg of conjugated/unconjugated C16 HC mixture was injected on column at decreasing relative percentages of conjugated C16 HC.

LC/MS/MS Analysis of Tryptic and Glu-C Digestion of ADC. ADCs (100 μg) were solubilized in 0.2% RapiGest (Waters Corp, 186001861) in 20 mM ammonium bicarbonate. The samples were then incubated at 80 °C for 15 min. Dithiothreitol (DTT, 20 mM final concentration) was added to the samples and incubated at 60 °C for 30 min to reduce disulfide bonds. After the samples were cooled to room temperature, iodoacetamide (IAA, 15 mM final concentration) was added and then samples were incubated at room temperature for 30 min in the dark to alkylate reduced cysteines. Modified trypsin or GluC (Promega, cat #V5111 or cat #V1651) was added (1:100 enzyme/substrate) and the samples were incubated at 37 °C overnight. To hydrolyze the RapiGest prior to mass spectrometry analysis, TFA was added to a final concentration of 60 mM, and the solution was incubated at 37 °C for 45 min, and then centrifuged at 20 800 *g* at 4 °C for 30 min. Samples (2.5 μg of digested protein) were loaded into a Agilent Poroshell 120 C18 column (2.1 × 100 mm, 2.7 μm) and eluted at 45 °C with a flow rate of 0.3 mL/min. LC/MS/MS analysis was performed using Agilent 1100 series HPLC system, coupled to an Orbitrap velos pro (Thermo Scientific) mass spectrometer with electrospray ion source. Peptides were separated by gradient elution using water as mobile phase A and acetonitrile as mobile phase B, both in 0.1% formic acid. The gradient elution used was as follows: 0−2 min 3% B; 2−85 min 3−50% B; 83−83.1 min 50−95% B; 83.1−85 min 95% B; 85−85.1 min 95−3% B; and 85.1−90 min 3% B. The Orbitrap Velos was operated in information dependent acquisition (IDA) mode with CID performed on the top 10 ions. The MS scan was performed in the orbitrap at 100 000 resolution whereas the fragment spectra were collected in the low pressure trap. Ion trap and orbitrap maximal injection times were set to 50 and 500 ms, respectively. The ion target values were 30 000 for the ion trap and 1 000 000 for the orbitrap.

Peptide Mass Fingerprint. The high resolution precursor ion MS data was deconvoluted using Xtract software (Thermo Scientific) to create a precursor peak list. The peptide mass fingerprint analysis was performed using Mascot software. The database search considered the monoisotopic mass of the peptide with a mass tolerance of ±0.03 Da. and no peptide missed cleavage. The database included the yeast proteome and the sequence of the antibody of interest. Carbamidomethylation of cysteines was searched as a fixed modification while deamidation and the delta mass that the payload conferred to the peptide (1089.65 Da for AmPEG6-MMAD) was searched as a variable modification. The reported proteins had a significance threshold of $p < 0.01$.

Protein Purification. Anti M1S1 antibodies were cloned into in-house expression plasmids. Protein was transiently expressed from HEK293 cells using standard procedures. C16 LC and C16 LC HC have two glycines before the glutamine tag (LLQGA) in the C-terminus of the light chain. The heavy chain of C16 LC has a K222R mutation in the heavy chain. Conditioned media was applied to Protein-A MabSelectSURE columns (GE Healthcare, Inc.) and washed with 140 mM NaCl, 2.7 mM KCl, and 10 mM PO_4^{-3} (1× phosphate buffered saline) until baseline was reached. Protein was eluted with 100 mM sodium citrate buffer, pH 3.5, and immediately neutralized with 800 mM sodium phosphate buffer, pH 7.4. Eluted protein was dialyzed into 1× phosphate buffered saline and stored at 4 °C.

Peptide Standard Conjugation. C16 LC, C16 HC, and Q295 peptide tags were dissolved at 10 mg/mL in 1% DMSO and diluted to 1 mg/mL in buffer containing 25 mM Tris-HCl at pH 8.0 and 150 mM NaCl. AmPEG6-Propionyl-MMAD was added at a 2.5-fold molar excess over peptide and the enzymatic reaction initiated by addition of 1% (w/v) mTG. The mixture incubated at 22 °C for 2 h prior to use.

Conjugated Peptides Detection Limit. The detection limit of C16 LC, C16 HC, and Q295 conjugated standard peptides was determined by serial dilution (1:5) of the peptides in the context of its corresponding unconjugated antibody tryptic digest (2.5 μg injected on column). The peptide abundance was measured as the area under the curve (AUC) of extracted chromatogram corresponding to the most intense molecular ion for each peptide (+2 for C16 LC, C16 HC and +3 for Q295). The peptide detection limit was defined as amount of peptide at which the peptide mass fingerprint analysis did not detect the conjugated peptide.

Hydrophobic Interaction and Size Exclusion Chromatography of ADCs. The relative distribution of conjugation products with different drug:antibody stoichiometries can be determined using hydrophobic interaction chromatography (HIC). ADCs with zero, one, or two drugs per antibody were separated using a TSKgel Butyl-NPR column (4.6 mm × 3.5 cm) (Tosoh Bioscience, King of Prussia, PA) on an Agilent HP 1100 HPLC (Agilent, Santa Clara, CA). The HIC method utilized a mobile phase of 1.5 M ammonium sulfate, 50 mM potassium phosphate at pH 7 for Buffer A, and 50 mM potassium phosphate, 15% isopropanol at pH 7 for Buffer B. Using a flow rate of 0.8 mL/min, 40 μg of ADC in 0.75 M ammonium sulfate was loaded onto the column and eluted with a gradient consisting of a 2.5 min hold at 0% B, followed by a 35 min linear gradient to 100% B. The column was washed with 100% Buffer B for 2.5 min and re-equilibrated with initial conditions for 5 min.

Aggregation was assessed by size exclusion chromatography. Antibody samples were diluted to 1 mg/mL in phosphate buffered saline, pH 7.4, and 15 μg injected onto a size exclusion KW-804 (7 μm, 8.0 × 300 mm, Shodex). The mobile phase

dx.doi.org/10.1021/bc4003794 | *Bioconjugate Chem.* 2014, 25, 240−250

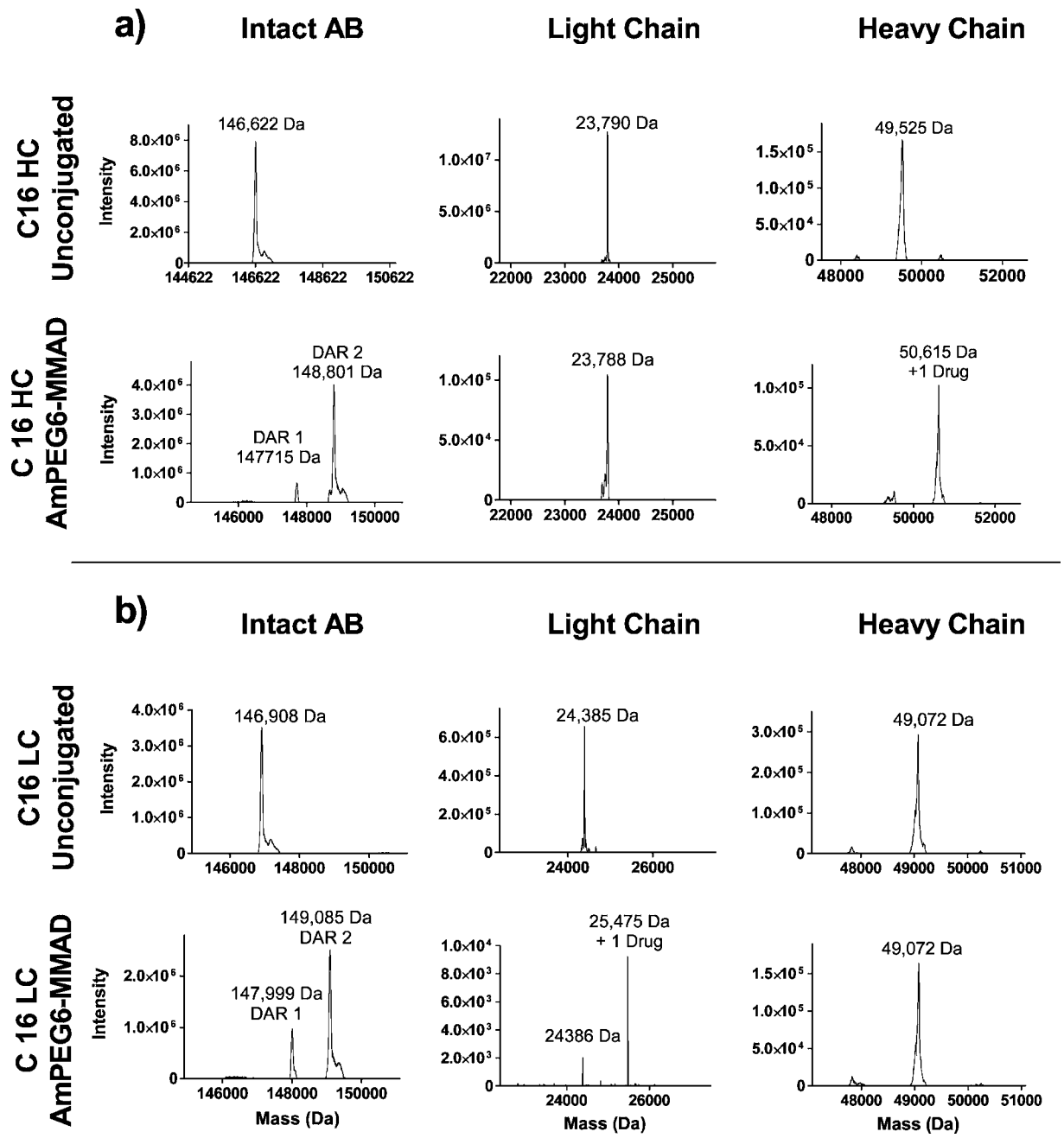

Figure 2. Intact mass of (a) C16 HC and (b) C16 LC unconjugated and conjugated to AmPEG6-MMAD (right column). The mass difference between unconjugated and 1 drug conjugated antibody (DAR 1) is 1089 Da, which corresponds to the mass of the cytotoxic drug. The mass difference between unconjugated and 2 drug conjugated antibody (DAR 2) is 2 × 1089 Da. The masses of the light chain and heavy chain of (a) C16 HC and (b) C16 LC unconjugated and conjugated are shown in the in the middle and left columns, respectively. C16 HC conjugated to one drug in the heavy chain, while C16 LC conjugated to a drug in the light chain.

consisted of 0.17 M potassium phosphate, pH 7.0, 0.21 M potassium chloride, 20% 2-propanol, running isocratically at a flow rate of 0.7 mL/min. The separation was monitored by absorbance at 280 nm.

Chemical Synthesis. AmPEG6-MMAD was synthesized as previously described.[17]

■ RESULTS AND DISCUSSION

To characterize the site-specificity of mTG technology, we selected a C16 antibody against M1S1 antigen with an engineered conjugation site in the heavy chain (C16 HC), light chain (C16 LC), and in both chains (C16 HC LC) (Figure 1c). For this study, we conjugated the C16 antibody with AmPEG6-MMAD: a noncleavable linker-payload. We utilized a combination of intact mass characterization, in-source fragment extracted chromatograms, and peptide fingerprinting coupled with standard curves to estimate the levels of site specificity.

Intact Mass Characterization. The intact mass of C16 HC and C16 LC (unconjugated and conjugated) are shown in Figure 2a and b. Relative to the corresponding unconjugated antibodies, C16 HC (upper panel, left column) and C16 LC (lower panel, left column) conjugates show an increase in molecular weight by either one or two AmPEG6-MMAD drugs

dx.doi.org/10.1021/bc4003794 | Bioconjugate Chem. 2014, 25, 240−250

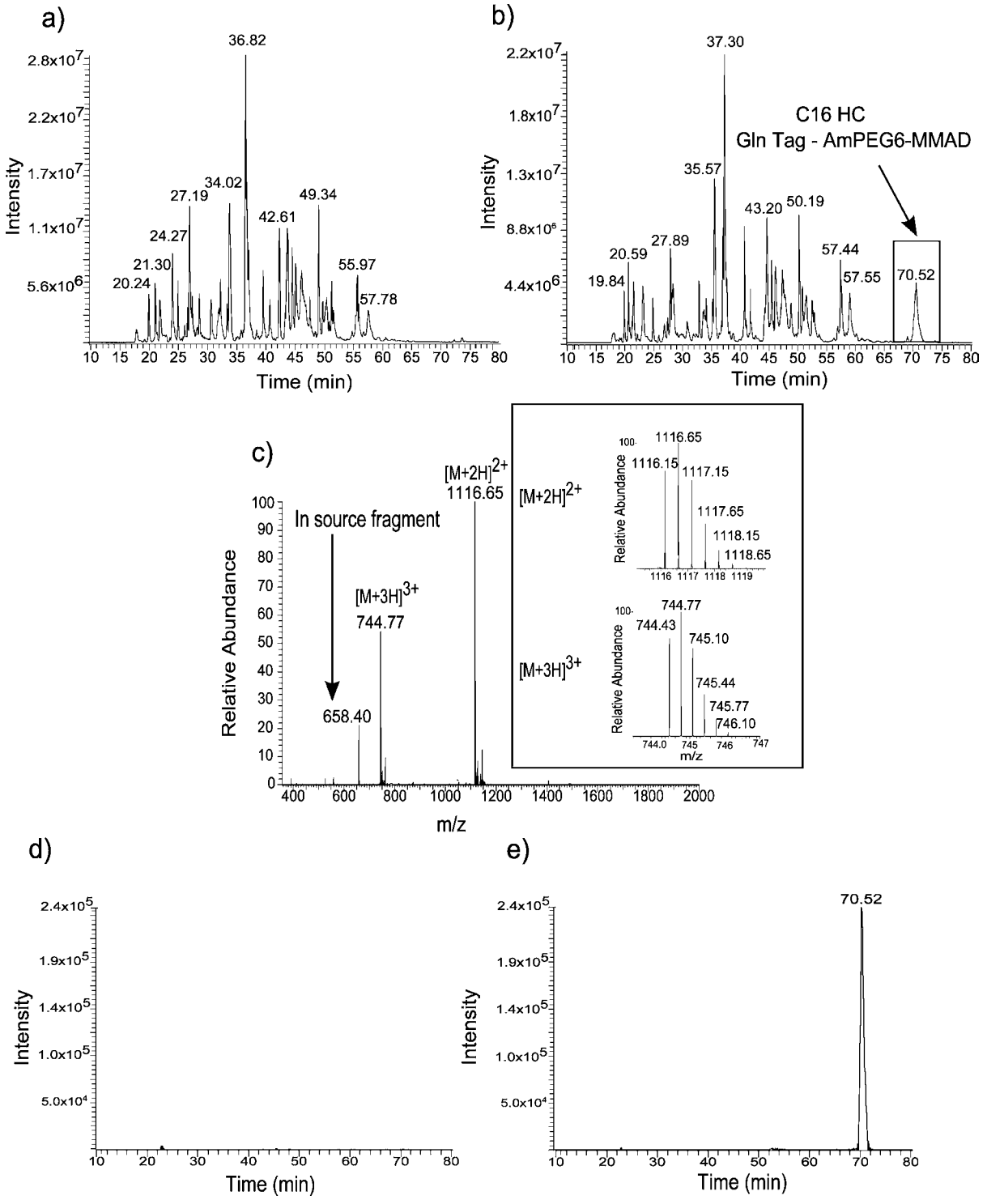

Figure 3. LC/MS chromatogram corresponding to (a) unconjugated and (b) AmPEG6-MMAD conjugated C16 HC tryptic digest. These two chromatograms show similar peptide elution profile except that there is a late eluting peptide (retention time 70.52 min) present in the conjugated C16 HC. MS spectra corresponding to retention time 70.52 min from conjugated C16 HC shows +2 and +3 molecular ions of AmPEG6-MMAD conjugated glutamine tag (SLSLSPGLLQ*GA) (c); this MS spectrum also shows the in-source fragment (m/z 658.40) characteristic of AmPEG6-MMAD containing peptides. The isotopically resolved +2 and +3 molecular ions are shown in c inset. The in-source fragment extracted chromatograms (m/z 658.4) for (d) unconjugated and (e) AmPEG6-MMAD conjugated C16 HC show a unique peak in the conjugated C16 HC that corresponded to the conjugated glutamine tag.

(1089 Da or 2 × 1089 Da). In both cases, most of the antibody is conjugated with two drugs while a small fraction is conjugated to only one drug. According to the intact mass analysis, both C16 HC and C16 LC show a maximum loading of two drugs per antibody with undetectable levels of higher-loaded species. The relative intensities of the drug antibody ratio (DAR) of 0, 1, and 2 can be used to calculate the drug loading of the ADC (Figure 2a and b, lower panel, left column).

dx.doi.org/10.1021/bc4003794 | Bioconjugate Chem. 2014, 25, 240−250

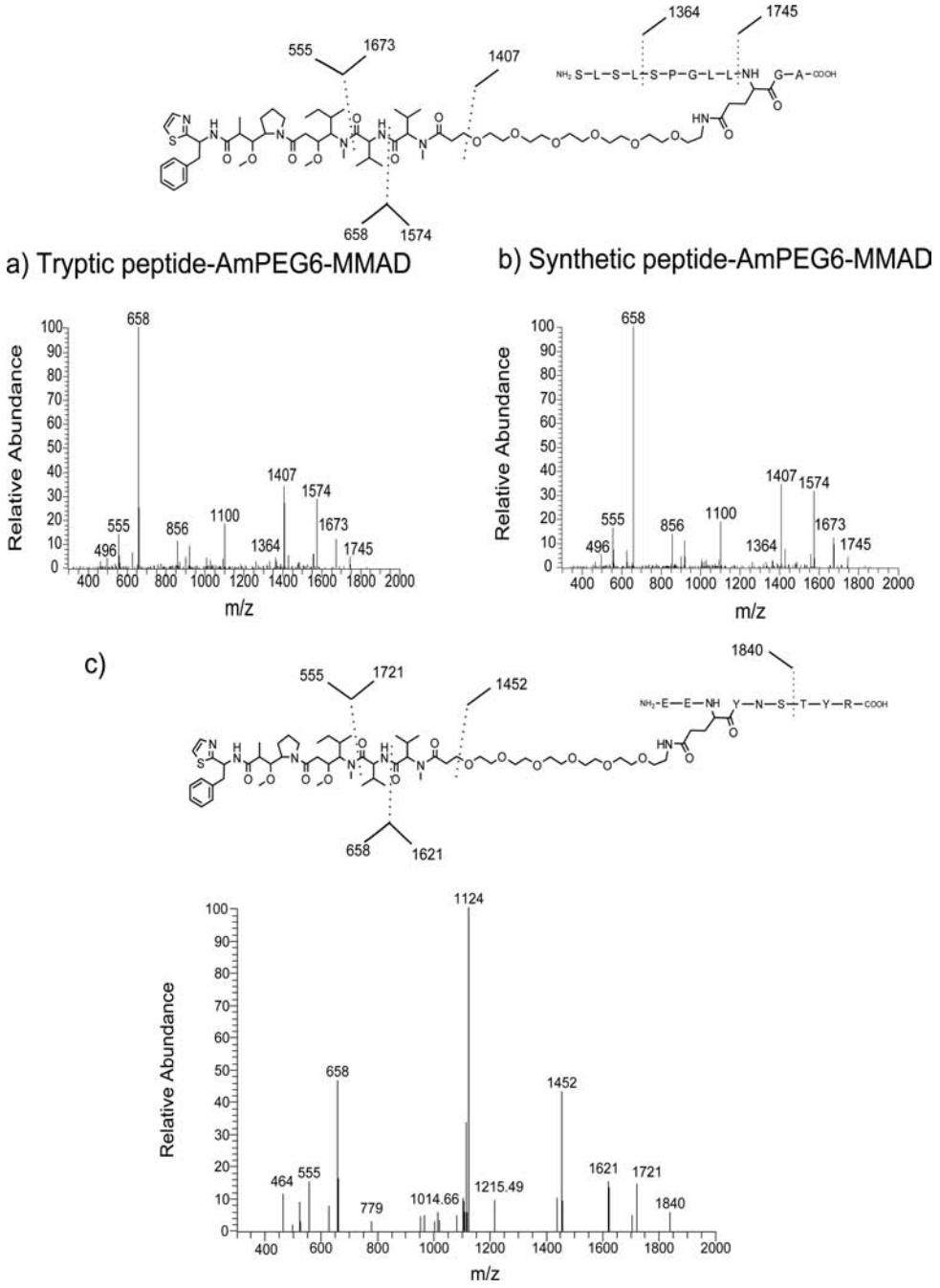

Figure 4. MS/MS spectrum of AmPEG6-MMAD conjugated to SLSLSPGLLQ*GA from (a) tryptic digestion of C16 HC and (b) AmPEG6-MMAD conjugated to SLSLSPGLLQ*GA synthetic peptide. The fragmentation of the +2 molecular ion (m/z 1116.65) corresponding to these two conjugated peptides (a, b) produced virtually identical spectra, and the resulting product ions matched the fragmentation of the molecule. MS/MS spectra from AmPEG6-MMAD conjugated to EEQ*YNSTYR from tryptic digestion of C16 HC (c). The ion m/z 1124 appears to be $[M+2H\text{-}MeOH]^{2+}$ often observed when the parent conjugated peptide loses CH3OH moiety from the payload during MS/MS acquisition. Drug conjugated peptides (a) SLSLSPGLLQ*GA and (c) EEQ*YNSTYR fragmented at the same positions in the MMAD portion of the molecule producing the identical fragmented ions m/z 658 and m/z 555.

Based on this calculation and a separate hydrophobic interaction chromatography (HIC) experiments (SI Figure S1), the DAR is 1.9 and 1.7 for C16 HC and C16 LC, respectively. Considering that the calculated drug loading by intact mass is in a good agreement with loading determined by our HIC method, we can assume that intact mass determination is a good approximation of drug loading.

Light and heavy chains of C16 HC and C16 LC were also characterized by LC/MS under reducing conditions (Figure 2). As expected for site-specific conjugation, we observed conjugation only to the heavy chain for C16 HC (upper panel, right column) and only to the light chain for C16 LC (lower panel, middle column, and SI Table S1). Since we did not observe any species with higher loading than 2.0 in either the C16 HC or C16 LC conjugates and we did not see any unexpected conjugations to the undesired antibody chains in the reduced samples, we can infer that most of our conjugation is site-specific.

dx.doi.org/10.1021/bc4003794 | *Bioconjugate Chem.* 2014, 25, 240−250

The intact mass characterization method utilized here is the least susceptible method to ionization efficiency differences (conjugation of AmPEG6-MMAD changes the molecular weight of intact antibody only by 1.5% of the total mass); however, it is also the least sensitive method used in this study. In an effort to estimate the detection limit of the intact mass analysis, we spiked decreasing amounts of AmPEG6-MMAD conjugated C16 HC into an unconjugated C16 HC, and monitored the DAR 2 peak (SI Figure S2). We found that the detection limit of DAR 2 was approximately 5% of the total mixture, suggesting that our conjugation specificity is better than 95%.

In-Source Fragment Ion Extracted Chromatogram. To test whether the drug conjugation using mTG is specific to the designed glutamine tag in the heavy chain, C16 HC was subjected to trypsin digestion and analyzed by LC/MS/MS (Figures 3 and 4). The chromatograms corresponding to the unconjugated C16 HC (Figure 3a) and C16 HC conjugated with AmPEG6-MMAD (Figure 3b) show comparable peptide elution profiles. The main difference is the presence of a late eluting peak in the conjugated C16 HC (retention time 70.52 min; Figure 3b). It has been previously reported that auristatin conjugated peptides have increase hydrophobicity and tend to elute at higher organic percentage than its nonconjugated counterpart.[22] The MS spectrum corresponding to retention time 70.52 min is shown is Figure 3c. The +2 and +3 molecular ions (m/z 1116.65 and 744.77, respectively) match the expected precursor ions of SLSLSPGLLQ*GA tryptic peptide containing the glutamine tag conjugated to AmPEG6-MMAD (Figure 3c). This MS spectrum also shows an in-source fragment (m/z 658.40) characteristic of AmPEG6-MMAD conjugated peptides. A similar in-source fragmentation was previously reported for the mc-vc-PABC-MMAE drug.[22]

To analyze the AmPEG6-MMAD containing peptides we took advantage of this characteristic in-source fragment (m/z 658.40) produced by the cleavage of the peptide bond at the N-terminus of MMAD molecule (Figure 4). The extracted chromatograms of MMAD characteristic ion are shown in Figure 3d and e for unconjugated and conjugated C16 HC, respectively. The conjugated sample shows a unique peak that corresponds to SLSLSPGLLQ*GA tryptic peptide containing the glutamine tag conjugated to AmPEG6-MMAD as previously determined.

The LC/MS trace of unconjugated and conjugated C16 LC is shown in SI Figure S3a and S3b, respectively. Once again, the conjugated peptides elutes at high organic due to their increased hydrophobicity. The extracted chromatograms of the MMAD characteristic in-source fragment ion of the unconjugated and conjugated C16 LC are shown in SI Figure S3c and S3d. In the case of the C16 LC, two peaks corresponding to the AmPEG6-MMAD conjugated peptides were found. Both peaks correspond to peptides containing the designed glutamine tag. The larger peak corresponds to the tryptic peptide GECGGLLQ*GA conjugated with AmPEG6-MMAD and the smaller peak corresponds to its missed cleavage conjugated peptide (SFNRGECGGLLQ*GA). MS spectra corresponding to retention time 67 min from the conjugated C16 LC (e) shows the +2 and +3 molecular corresponding to AmPEG6-MMAD conjugated to GECGGLLQ*GA.

Peptide Mass Fingerprinting. LC/MS data acquisition of the unconjugated and conjugated C16 HC tryptic digests was performed in an Obitrap Velos Pro (Thermo Scientific) operated at high resolution (100 000) and the peptide mass fingerprint data was analyzed with Mascot. The database was searched considering delta mass that the payload conferred to the peptide (1089.65 Da for AmPEG6-MMAD) as a variable modification of glutamine residues with a tolerance of 0.03 Da. The sequence coverage of unconjugated and conjugated C16 HC tryptic digests were 94% and 95%, respectively, and covered all glutamine residues within the antibody sequence. As expected, no modification was found in the unconjugated C16 HC. The analysis of conjugated C16 HC confirmed the conjugation of the tryptic peptide containing the engineered glutamine tag in the C-terminus of the heavy chain (SLSLSPGLLQ*GA). The identity of this drug−peptide conjugate was verified by comparing the peptide's MS/MS spectra to the spectra of a synthetic SLSLSPGLLQ*GA peptide standard which was conjugated with AmPEG6-MMAD (Figure 4a and b. respectively). To our knowledge this is the first time that the MS/MS of a peptide−linker−monomethyl auristatin D is described. The collision induced dissociation (CID) fragmentation of the +2 molecular ion (m/z 1116.65) corresponding to these two conjugated peptides produced virtually identical spectra, and the resulting product ions matched the fragmentation of the molecule (see molecular structure in Figure 4). The MS/MS of the glutamine peptide tag conjugated to AmPEG6-MMAD reveals a spectrum dominated by fragmentation of amide bonds in the MMAD portion of the molecule (including the in-source fragment (m/z 658.40) and few b and y ions from the peptide portion). For this reason, the analysis of conjugation sites is not suitable for typical MS/MS database search, as the conjugated peptide produces low scoring matches.

Similar to the C16 HC, the peptide mass fingerprint sequence coverage of unconjugated and conjugated C16 LC tryptic digest was 95% and 96%, respectively, with full coverage of all glutamine residues. The peptide mass fingerprint analysis of the conjugated C16 LC tryptic digest confirmed the conjugation of AmPEG6-MMAD to the light chain glutamine tag peptide GECGGLLQ*GA and a missed cleavage of the same peptide SFNRGECGGLLQ*GA. The identity of peptide−drug conjugate was verified by comparison of the MS/MS spectra to synthetic peptide GECGGLLQ*GA conjugated with AmPEG6-MMAD (SI Figure S4a and S4b, respectively). The CID fragmentation of the +2 molecular ion (m/z 1026.05) produced identical spectrum to the conjugated synthetic peptide and the resulting product ions matched the fragmentation of the molecule at multiple locations. The identity of the missed cleavage peptide SFNRGECGGLLQ*-GA was also verified by MS/MS (SI Figure S4c). The peptide mass fingerprint results for conjugated C16 LC and C16 HC tryptic digest were also reproduced using Glu-C enzymatic digestion (data not shown).

Specificity of mTG Conjugation. In addition to the expected designed conjugation sites, peptide mass fingerprint analysis also revealed that the tryptic peptide EEQ*YNSTYR was conjugated to AmPEG6-MMAD in both C16 HC as well as in C16 LC. EEQ*YNSTYR conjugated peptide eluted at 59 min from the HPLC column. The identity of the EEQ*YN-STYR AmPEG6-MMAD conjugated peptide was confirmed by MS/MS (Figure 4c and SI Figure S4d). The product ion spectrum specific to +3 molecular ion (m/z 760.39) was consistent with the fragmentation of EEQ*YNSTYR conjugated to AmPEG6-MMAD (Figure 4c, structural inset). This tryptic peptide is located in the CH2 region of the heavy chain

dx.doi.org/10.1021/bc4003794 | Bioconjugate Chem. 2014, 25, 240−250

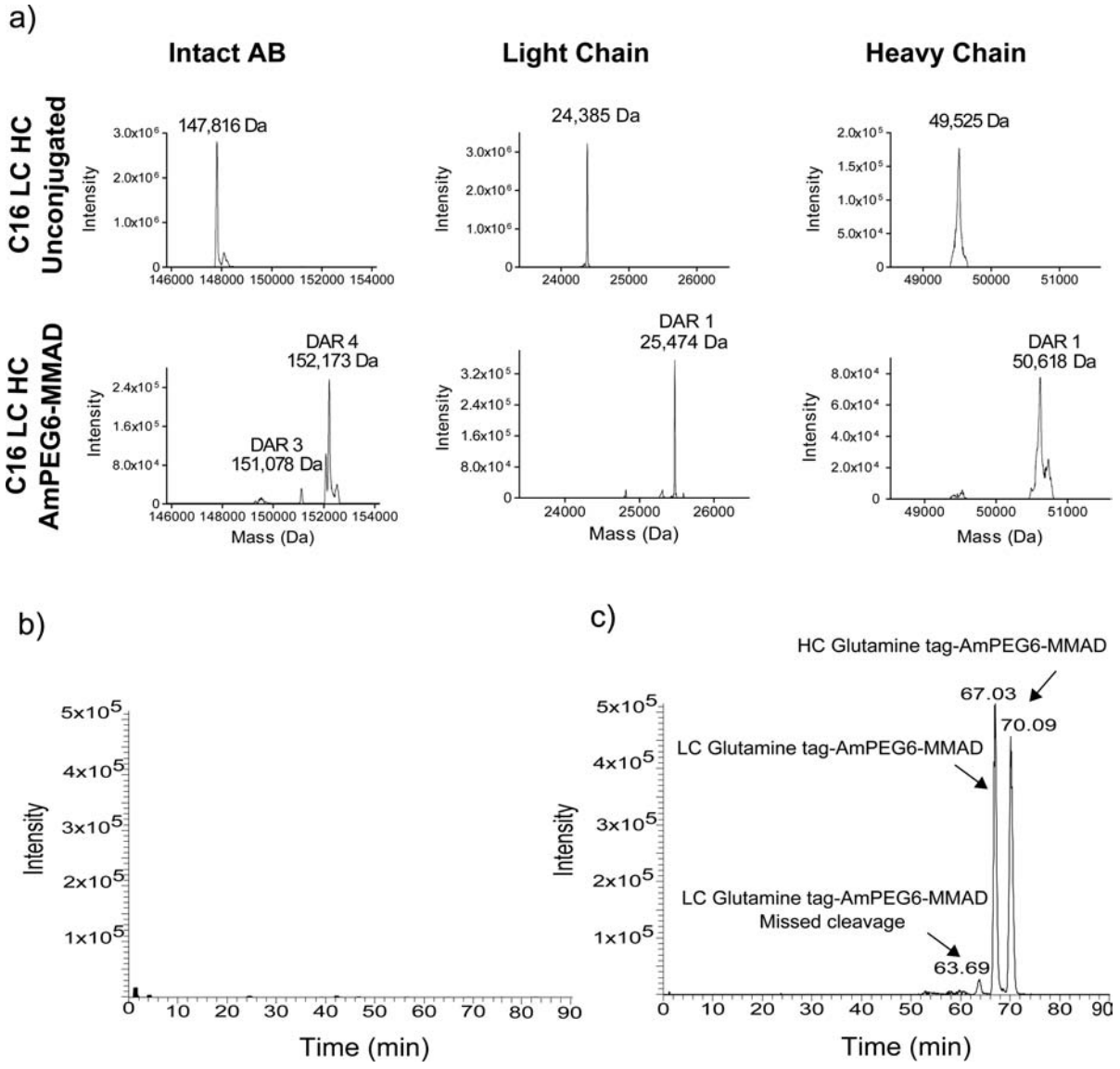

Figure 5. Intact mass deconvolution of C16 LC HC unconjugated and conjugated to AmPEG6-MMAD (a, first column). Conjugated C16 LC HC is either 3 × 1089 Da or 4 × 1089 Da heavier than its correspondent unconjugated counter pair. The masses of the light chain and heavy chain of C16 LC HC (unconjugated and conjugated) are shown in the middle and right column, respectively. C16 HC LC conjugates to one drug in the heavy chain and light chain. In-source fragment (m/z 658.4) extracted chromatogram corresponding to unconjugated (b) and AmPEG6- MMAD conjugated (c) C16 LC HC.

and encompasses the Fc glycosylation site N297. It has been reported that mTG can recognize Q295 in deglycosylated IgGs and conjugation can be achieved at this site.[26] When antibodies are expressed in CHO or HEK293 expression systems, most of the produced proteins are glycosylated at position N297. The presence of glycans at position N297 prevents conjugation to Q295. However, there is typically a small fraction of aglycosylated antibodies that are also produced. It is this contaminating aglycosylated antibody fraction, which is suitable for conjugation at position Q295. The identified EEQYN sequence does not resemble the LLQGA glutamine tag that we selected for conjugation, suggesting that transglutaminase has somewhat promiscuous sequence specificity. The conjugation specificity of transglutaminase has been studied previously[29−31] and the data suggest that, in addition to sequence preference, conjugation by transglutaminase depends on the local three-dimensional structure and enzyme accessibility.

To estimate the amount of this off-target conjugation to Q295 site, we spiked conjugated EEQ*YNSTYR standard peptide into a fixed amount (2.5 μg) of unconjugated tryptic digests of C16 HC and generated a standard curve for quantification. Using the precursor ion extracted chromatogram, we were able to estimate that 1.3% of the total injected Q295 peptide is conjugated with AmPEG6-MMAD in the C16 HC molecule assuming 100% digestion efficiency (SI Figure S5a). The conjugated EEQ*YNSTYR peptide (elution time 59 min) is not clearly visible in the m/z 658.4 extracted chromatogram (Figure 3e, and SI Figure S3d). The spike-in experiments verified that the sensitivity of the m/z 658.4 in-source fragment ion extracted chromatogram method was approximately 2% under these conditions (5σ cutoff), which is why we could not identify the EEQ*YNSTYR conjugated peptide in the in-source fragment extracted chromatograms.

dx.doi.org/10.1021/bc4003794 | *Bioconjugate Chem.* 2014, 25, 240−250

Elimination of Conjugation Byproducts. Although the majority of the drug conjugated to the designed glutamine tag, we found an off-target glutamine conjugation at the Q295. To further improve homogeneity of the ADCs we created a single point mutant Q295N to abolish the undesired conjugation. As expected, the peptide mass fingerprint of the Q295N mutant revealed only conjugation at the designed glutamine tag site for both C16 LC and C16 HC molecules with no additional identified sites.

The conjugated peptide detection limits were determined by its serial dilution into a fixed amount of unconjugated antibody tryptic digest (SI Figure S5). The detection limit for AmPEG6-MMAD conjugated peptides EEQ*YNSTYR (Q295), SLSLSPGLLQ*GA (C16 HC), and GECGGLLQ*GA (C16 LC) was 69, 71, and 5 fmol injected on column, respectively (SI Figure 5 a,b,c), corresponding to between 0.01% and 0.2% of the total injected peptides (assuming 100% digestion efficiency). This detection limit was defined as the amount of peptide at which the peptide mass fingerprint analysis did not detect the conjugated peptide. The absolute detection limit based on ion intensity was much lower (0.5, 2.6, and 14 fmol, respectively) than the detection limit of the entire method, which does not require manual interpretation of the spectra.

Site Specificity of mTG Conjugation Reaction. Since we do not detect any off-target conjugated peptides in the C16 HC Q295N conjugate by any of the methods presented here, it is difficult to estimate the purity of the conjugate with extreme levels of accuracy. Based on the intact mass measurements and extracted in-source fragment ion, the C16 HC Q295N conjugate is better than 95−98% site-specific. The most sensitive method used in this study was the peptide mass fingerprinting coupled with MS/MS. We found the detection limit of the three identified peptides to be between 0.01% and 0.2% of the total injected peptides. Due to the differences in conjugated peptide ionization it is not possible to precisely determine the detection limit of this method. However, if we assume that the three conjugated peptides are good representatives of other potentially conjugated peptides, then the C16 HC Q295N conjugate would be better than 99.8% site-specific.

Characterization of Higher Loaded Conjugates. We also wanted to test whether the MS characterization described here would be applicable to higher loaded species. To that end, we generated an antibody that carried simultaneously the HC and LC glutamine tags. The intact mass of C16 LC HC (unconjugated and conjugated) is shown in Figure 5a, first column. Most of the ADC is conjugated with four drugs while a smaller fraction is conjugated to three drugs resulting in DAR of 3.8 as calculated by HIC chromatography and intact mass analysis. As expected, in the reduced samples both the light and heavy chain of C16 LC HC showed conjugation to one drug (Figure 5a, second and third columns).

In-source MMAD fragment extracted chromatograms of the unconjugated and conjugated C16 LC HC (Figure 5b and c) show two major late eluting conjugated peptides in the conjugated tryptic digest (Figure 5c). The elution times of these two peptides were identical to the C16 HC and C16 LC conjugated samples (Figure 3e and SI Figure S3d). The identity of these peptides was also verified by MS/MS analysis (data not shown). These results plus peptide mass fingerprint confirmed the site-specific conjugation of the glutamine tags in the C16 LC HC antibody, and showed that the methods presented here can be applied to ADCs that contain more than one site-specific site.

The in-source fragmentation of auristatins linked to peptides has been previously described.[22,32] Junutula et al. used the in-source fragment (m/z 718.5) extracted chromatogram to visually characterize MC-vc-PABC-MMAE containing mass spectra in a tryptic digest of an ADC (THIOMAB, Thio-3A5). Alley et al. also reported the in-source fragment (m/z 619.4) in the collision induced dissociation of a tryptic peptide (T6) from rat serum albumin conjugated to mc-MMAF. In both cases, in-source fragmentation was used for qualitative examination and identification of peptide−auristatin conjugates. In our report, we used the in-source fragment not only for qualitative characterization but also to establish limits of quantitation of the site-specific conjugation produced by transglutaminase technology. While the in-source fragmentation of auristatins is a helpful tool to identify conjugated peptides, this approach might not be applicable to all cytotoxic drugs since some might not produce it.

Identification of post-translational modification site is typically achieved by LC/MS/MS experiment followed by database search. While this approach can work for some ADCs, the collision induced dissociation of peptide-AmPEG6-MMAD conjugate produced spectrum dominated by fragmentation of the payload, yielding very low scoring peptides when using a database search analysis. This made the use of MS/MS data acquisition unreliable for the identification of conjugation sites.

To circumvent these limitations, we developed a general method to identify conjugation sites in antibody−drug conjugates. This method consists of high-resolution LC/MS data acquisition followed by a database search of the deconvoluted precursor ion masses. In this search, we use the delta mass of the drug to identify conjugation sites and obtain specificity by the low tolerance allowed in the search (0.03 Da). This approach is compatible with commercially available software such as MASCOT. To the best of our knowledge, no tools to quantify conjugation site specificity of antibody−drug conjugates have been published. In this report, we used peptide-payload standards to create standard curves that allowed us to quantify conjugation site and determine detection limit for low-level off-target conjugation.

In summary, LC/MS and LC/MS/MS analysis of C16 HC, C16 LC, and C16 LC HC antibody−drug conjugates reveals that mTG conjugation technology produces highly site-specific and homogeneous ADCs (Table 1). The mTG-based method for antibody−drug conjugation offers versatile and precise control over the site of conjugation and the drug:antibody ratio, allowing us to generate homogeneous conjugates in a reproducible manner. We identified an undesired conjugation site (Q295), which carried approximately 1.3% of the conjugated drug. In a typical antibody, the presence of glycans at position N297 prevents conjugation to Q295. However, during antibody expression a small fraction does not carry glycans and can therefore be conjugated at this position. We were able to eliminate this heterogeneity with the Q295N mutant, and show that once eliminated we do not detect any undesired conjugation site. We estimate the detection limit of the described process to be 0.01−0.2% based on our ability to detect minute amounts of several synthetic conjugated peptides spiked into samples of digested ADCs. If we assume that conjugated peptides used in this study are representative of other potentially conjugated peptides, then the C16 HC Q295N conjugate would be better than 99.8% site-specific. The

analytical methods presented here should not only be applicable to transglutaminse based conjugates, but also be generalizable for other site-specific conjugation techniques. As site-specific conjugation methods gain momentum for ADC production, it will be important to develop further methods with defined limits of detection for accurate quantification of low-level impurities that may arise in the course of a given conjugation.

■ ASSOCIATED CONTENT

Supporting Information

Hydrophobic interaction chromatography traces corresponding to C16 LC and C16 HC conjugates. Detection limit of C16 HC conjugate (intact mass). LC/MS analysis of C16 LC tryptic digests. MS/MS analysis of conjugated peptides corresponding to C16 LC tryptic digests. Standard curves of conjugated synthetic peptides. This material is available free of charge via the Internet at http://pubs.acs.org.

■ AUTHOR INFORMATION

Corresponding Author

*E-mail: pavel.strop@pfizer.com.

Author Contributions

Santiago E. Farias and Pavel Strop contributed equally to the work.

Notes

The authors declare no competing financial interest.

■ ACKNOWLEDGMENTS

We would like to thank Russell Dushin, Gary Filzen, Jim MacDonald, and Christopher O'Donnell for the synthesis of AmPEG6-MMAD. We would also like to thank Mike Sherman Chin, Teresa M. Wong, Ishita Barman, and Colleen Brown for cell culture support and Shu-Hui Liu, Kirk Hansen, Jeremy Myers, and James Carroll for discussions and reading of the manuscript.

■ ABBREVIATIONS

ADC, antibody drug conjugates; TG, Transglutaminase; AmPEG6MMAD, amino-polyethylene glycol-6 propionyl monomethyl auristatin D; LC, liquid chromatography; MS, mass spectrometry; MS/MS, tandem mass spectrometry; Fab, fragment antigen binding; HC, heavy chain; LC, light chain; DTT, dithiothreitol

■ REFERENCES

(1) Lambert, J. M. (2005) Drug-conjugated monoclonal antibodies for the treatment of cancer. *Curr. Opin. Pharmacol. 5*, 543−9.

(2) Senter, P. D. (2009) Potent antibody drug conjugates for cancer therapy. *Curr. Opin. Chem. Biol. 13*, 235−44.

(3) Junutula, J. R., Flagella, K. M., Graham, R. A., Parsons, K. L., Ha, E., Raab, H., Bhakta, S., Nguyen, T., Dugger, D. L., Li, G., Mai, E., Lewis Phillips, G. D., Hiraragi, H., Fuji, R. N., Tibbitts, J., Vandlen, R., Spencer, S. D., Scheller, R. H., Polakis, P., and Sliwkowski, M. X. (2010) Engineered thio-trastuzumab-DM1 conjugate with an improved therapeutic index to target human epidermal growth factor receptor 2-positive breast cancer. *Clin. Cancer Res. 16*, 4769−78.

(4) Senter, P. D., and Sievers, E. L. (2012) The discovery and development of brentuximab vedotin for use in relapsed Hodgkin lymphoma and systemic anaplastic large cell lymphoma. *Nat. Biotechnol. 30*, 631−7.

(5) Ricart, A. D., and Tolcher, A. W. (2007) Technology insight: cytotoxic drug immunoconjugates for cancer therapy. *Nat. Clin. Pract. Oncol. 4*, 245−55.

(6) Ducry, L., and Stump, B. (2010) Antibody-drug conjugates: linking cytotoxic payloads to monoclonal antibodies. *Bioconjugate Chem. 21*, 5−13.

(7) Doronina, S. O., Toki, B. E., Torgov, M. Y., Mendelsohn, B. A., Cerveny, C. G., Chace, D. F., DeBlanc, R. L., Gearing, R. P., Bovee, T. D., Siegall, C. B., Francisco, J. A., Wahl, A. F., Meyer, D. L., and Senter, P. D. (2003) Development of potent monoclonal antibody auristatin conjugates for cancer therapy. *Nat. Biotechnol. 21*, 778−84.

(8) Lambert, J. M. (2012) Drug-conjugated antibodies for the treatment of cancer. *Br. J. Clin. Pharmacol. 76*, 248−262.

(9) Wagner-Rousset, E., Janin-Bussat, M. C., Colas, O., Excoffier, M., Haeuw, J. F., Rilatt, I., Perez, M., Corvaia, N., and Beck, A. (2013) Antibody Drug Conjugate model fast characterization by LC-MS following IdeS proteolytic digestion. *mAbs 6*, DOI: 10.4161/mabs.26773.

(10) Kellogg, B. A., Garrett, L., Kovtun, Y., Lai, K. C., Leece, B., Miller, M., Payne, G., Steeves, R., Whiteman, K. R., Widdison, W., Xie, H., Singh, R., Chari, R. V., Lambert, J. M., and Lutz, R. J. (2011) Disulfide-linked antibody-maytansinoid conjugates: optimization of in vivo activity by varying the steric hindrance at carbon atoms adjacent to the disulfide linkage. *Bioconjugate Chem. 22*, 717−27.

(11) Flygare, J. A., Pillow, T. H., and Aristoff, P. (2013) Antibody-drug conjugates for the treatment of cancer. *Chem. Biol. Drug Des. 81*, 113−21.

(12) Wang, L., Amphlett, G., Blattler, W. A., Lambert, J. M., and Zhang, W. (2005) Structural characterization of the maytansinoid-monoclonal antibody immunoconjugate, huN901-DM1, by mass spectrometry. *Protein Sci. 14*, 2436−46.

(13) Alley, S. C., and Anderson, K. E. (2013) Analytical and bioanalytical technologies for characterizing antibody-drug conjugates. *Curr. Opin. Chem. Biol. 17*, 406−411.

(14) Shen, B. Q., Xu, K., Liu, L., Raab, H., Bhakta, S., Kenrick, M., Parsons-Reponte, K. L., Tien, J., Yu, S. F., Mai, E., Li, D., Tibbitts, J., Baudys, J., Saad, O. M., Scales, S. J., McDonald, P. J., Hass, P. E., Eigenbrot, C., Nguyen, T., Solis, W. A., Fuji, R. N., Flagella, K. M., Patel, D., Spencer, S. D., Khawli, L. A., Ebens, A., Wong, W. L., Vandlen, R., Kaur, S., Sliwkowski, M. X., Scheller, R. H., Polakis, P., and Junutula, J. R. (2012) Conjugation site modulates the in vivo stability and therapeutic activity of antibody-drug conjugates. *Nat. Biotechnol. 30*, 184−9.

(15) Boswell, C. A., Mundo, E. E., Zhang, C., Bumbaca, D., Valle, N. R., Kozak, K. R., Fourie, A., Chuh, J., Koppada, N., Saad, O., Gill, H., Shen, B. Q., Rubinfeld, B., Tibbitts, J., Kaur, S., Theil, F. P., Fielder, P. J., Khawli, L. A., and Lin, K. (2011) Impact of drug conjugation on pharmacokinetics and tissue distribution of anti-STEAP1 antibody-drug conjugates in rats. *Bioconjugate Chem. 22*, 1994−2004.

(16) Kozak, K. R., Tsai, S. P., Fourie-O'Donohue, A., Dela Cruz Chuh, J., Roth, L., Cook, R., Chan, E., Chan, P., Darwish, M., Ohri, R., Raab, H., Zhang, C., Lin, K., and Wong, W. L. (2013) Total antibody quantification for MMAE-conjugated antibody-drug conjugates: impact of assay format and reagents. *Bioconjugate Chem. 24*, 772−779.

(17) Strop, P., Liu, S. H., Dorywalska, M., Delaria, K., Dushin, R. G., Tran, T. T., Ho, W. H., Farias, S., Casas, M. G., Abdiche, Y., Zhou, D., Chandrasekaran, R., Samain, C., Loo, C., Rossi, A., Rickert, M., Krimm, S., Wong, T., Chin, S. M., Yu, J., Dilley, J., Chaparro-Riggers, J., Filzen, G. F., O'Donnell, C. J., Wang, F., Myers, J. S., Pons, J., Shelton, D. L., and Rajpal, A. (2013) Location matters: site of conjugation modulates stability and pharmacokinetics of antibody drug conjugates. *Chem. Biol. 20*, 161−7.

(18) McDonagh, C. F., Turcott, E., Westendorf, L., Webster, J. B., Alley, S. C., Kim, K., Andreyka, J., Stone, I., Hamblett, K. J., Francisco, J. A., and Carter, P. (2006) Engineered antibody-drug conjugates with defined sites and stoichiometries of drug attachment. *Protein Eng. Des. Sel. 19*, 299−307.

(19) Sun, M. M., Beam, K. S., Cerveny, C. G., Hamblett, K. J., Blackmore, R. S., Torgov, M. Y., Handley, F. G., Ihle, N. C., Senter, P.

D., and Alley, S. C. (2005) Reduction-alkylation strategies for the modification of specific monoclonal antibody disulfides. *Bioconjugate Chem. 16*, 1282−90.
(20) Jeffrey, S. C., Burke, P. J., Lyon, R. P., Meyer, D. W., Sussman, D., Anderson, M., Hunter, J. H., Leiske, C. I., Miyamoto, J. B., Nicholas, N. D., Okeley, N. M., Sanderson, R. J., Stone, I. J., Zeng, W., Gregson, S. J., Masterson, L., Tiberghien, A. C., Howard, P. W., Thurston, D. E., Law, C. L., and Senter, P. D. (2013) A potent anti-CD70 antibody-drug conjugate combining a dimeric pyrrolobenzodiazepine drug with site-specific conjugation technology. *Bioconjugate Chem. 24*, 1256−1263.
(21) Kung Sutherland, M. S., Walter, R. B., Jeffrey, S. C., Burke, P. J., Yu, C., Kostner, H., Stone, I., Ryan, M. C., Sussman, D., Lyon, R. P., Zeng, W., Harrington, K. H., Klussman, K., Westendorf, L., Meyer, D., Bernstein, I. D., Senter, P. D., Benjamin, D. R., Drachman, J. G., and McEarchern, J. A. (2013) SGN-CD33A: a novel CD33-targeting antibody-drug conjugate utilizing a pyrrolobenzodiazepine dimer is active in models of drug-resistant AML. *Blood 122*, 1455−1463.
(22) Junutula, J. R., Raab, H., Clark, S., Bhakta, S., Leipold, D. D., Weir, S., Chen, Y., Simpson, M., Tsai, S. P., Dennis, M. S., Lu, Y., Meng, Y. G., Ng, C., Yang, J., Lee, C. C., Duenas, E., Gorrell, J., Katta, V., Kim, A., McDorman, K., Flagella, K., Venook, R., Ross, S., Spencer, S. D., Lee Wong, W., Lowman, H. B., Vandlen, R., Sliwkowski, M. X., Scheller, R. H., Polakis, P., and Mallet, W. (2008) Site-specific conjugation of a cytotoxic drug to an antibody improves the therapeutic index. *Nat. Biotechnol. 26*, 925−32.
(23) Axup, J. Y., Bajjuri, K. M., Ritland, M., Hutchins, B. M., Kim, C. H., Kazane, S. A., Halder, R., Forsyth, J. S., Santidrian, A. F., Stafin, K., Lu, Y., Tran, H., Seller, A. J., Biroc, S. L., Szydlik, A., Pinkstaff, J. K., Tian, F., Sinha, S. C., Felding-Habermann, B., Smider, V. V., and Schultz, P. G. (2012) Synthesis of site-specific antibody-drug conjugates using unnatural amino acids. *Proc. Natl. Acad. Sci. U.S.A. 109*, 16101−6.
(24) Ohtsuka, T., Sawa, A., Kawabata, R., Nio, N., and Motoki, M. (2000) Substrate specificities of microbial transglutaminase for primary amines. *J. Agric. Food Chem. 48*, 6230−3.
(25) Yokoyama, K., Nio, N., and Kikuchi, Y. (2004) Properties and applications of microbial transglutaminase. *Appl. Microbiol. Biotechnol. 64*, 447−54.
(26) Jeger, S., Zimmermann, K., Blanc, A., Grunberg, J., Honer, M., Hunziker, P., Struthers, H., and Schibli, R. (2010) Site-specific and stoichiometric modification of antibodies by bacterial transglutaminase. *Angew. Chem., Int. Ed. Engl. 49*, 9995−7.
(27) Sato, H. (2002) Enzymatic procedure for site-specific pegylation of proteins. *Adv. Drug Delivery Rev. 54*, 487−504.
(28) Dai, L., Preston, R., Bacica, M., Kinhikar, A., Bolaños, B., and Murphy, R. E. (2012) Development of a potential high-throughput workflow to characterize sites of bioconjugation by immuno-affinity capture coupled to MALDI-TOF mass spectrometry. *Bioconjugate Chem. 24*, 53−62.
(29) Vanderlinden, L. A., Saba, L. M., Kechris, K., Miles, M. F., Hoffman, P. L., and Tabakoff, B. (2013) Whole brain and brain regional coexpression network interactions associated with predisposition to alcohol consumption. *PloS One 8*, e68878.
(30) Hafko, R., Villapol, S., Nostramo, R., Symes, A., Sabban, E. L., Inagami, T., and Saavedra, J. M. (2013) Commercially available angiotensin II At2 receptor antibodies are nonspecific. *PLoS One 8*, e69234.
(31) Moskvina, V., Harold, D., Russo, G., Vedernikov, A., Sharma, M., Saad, M., Holmans, P., Bras, J. M., Bettella, F., Keller, M. F., Nicolaou, N., Simon-Sanchez, J., Gibbs, J. R., Schulte, C., Durr, A., Guerreiro, R., Hernandez, D., Brice, A., Stefansson, H., Majamaa, K., Gasser, T., Heutink, P., Wood, N., Martinez, M., Singleton, A. B., Nalls, M. A., Hardy, J., Owen, M. J., O'Donovan, M. C., Williams, J., Morris, H. R., and Williams, N. M. (2013) Analysis of genome-wide association studies of Alzheimer disease and of Parkinson disease to determine if these 2 diseases share a common genetic risk. *JAMA Neurol. 70*, 1268−1276.
(32) Alley, S. C., Benjamin, D. R., Jeffrey, S. C., Okeley, N. M., Meyer, D. L., Sanderson, R. J., and Senter, P. D. (2008) Contribution of linker stability to the activities of anticancer immunoconjugates. *Bioconjugate Chem. 19*, 759−65.